International Journal of Mechanical, Industrial and Aerospace Sciences
ISSN: 2517-9950
Vol:6, No:10, 2012

An Analytical Solution for Vibration of Elevator Cables with Small Bending Stiffness

R. Mirabdollah Yani, E. Darabi

***Abstract*—**Responses of the dynamical systems are highly affected by the natural frequencies and it has a huge impact on design and operation of high-rise and high-speed elevators. In the present paper, the variational iteration method (VIM) is employed to investigate better understanding the dynamics of elevator cable as a single-degree-of-freedom (SDOF) swing system. Comparisons made among the results of the proposed closed-form analytical solution, the traditional numerical iterative time integration solution, and the linearized governing equations confirm the accuracy and efficiency of the proposed approach. Furthermore, based on the results of the proposed closed-form solution, the linearization errors in calculating the natural frequencies in different cases are discussed.

***Keywords*—**variational iteration method (VIM); cable vibration; closed-form solution

I. Introduction

CABLES are the structural elements of diverse engineering applications and are utilized in many machines and apparatuses. Cables and ropes resist relatively large axial loads, thus they are widely used in towing operations to carry and transmit high loads such as elevators, suspension bridges and marine towing systems. High flexibility and low intrinsic damping are the most important reason of cable vibrations. Mechanical properties of cables have been studied by many researchers. Stevin in 1586 instituted the triangle of forces by experimenting with loaded string, Beeckman in 1615 solved the suspension bridge problem, and John Bernoulli and James between 1690 and 1691 established the foundation of the catenary theory[1].

Several researchers studied the vibration of elevator cables. Chi and Shu calculated the natural frequencies of longitudinal vibration of a stationary cable and car system[2]. Yamamoto et al. analyzed the free and forced lateral vibration of a stationary string with slowly, linearly varying length[3]. Terumichi et al. examined the lateral vibration of a travelling string with slowly, linearly varying length and a mass-spring termination[4]. Zhu and Xu studied the vibration of elevator cables with small bending stiffness with different boundary conditions[5].

Vibration of hoist cable is a well known nonlinear problem. Exact solution of nonlinear equations is the most critical concern of researchers and mathematicians. Interpretation of a nonlinear phenomena is largely depends on these solutions.

R. Mirabdollah Yani is with the Damavand University of Applied Science and Technology, Iran (phone: +98 912 1480092; e-mail: Yani@damavand-uast.ac.ir).

E.Darabi is with the Damavand University of Applied Science and Technology, Irana (phone: +989122601628; e-mail: Ehsan.darabi@live.com).

The Variational Iteration Method (VIM)-proposed by Jin-Huan He in 1999-has been extensively used by arbitrary number of authors due to its flexibility and accuracy. Variational iteration method is a simple and efficient procedure for finding a solution of various nonlinear problems. Recently, virtues of the method attract engineers to utilize it in most of sophisticated fields. Numerous studies have been made in the area of vibration problems and new techniques was developed such as finite element method, finite difference method, perturbation techniques and etc to handle a more exact solution[6].

II. Analysis

A. Basic Equations for Stationary Cable Models

Consider three models of stationary hoist cable with different boundary conditions. Fig.1 shows these three models. In Fig.1a and Fig.1b, since there is no sag, a taut string and a tensioned beam are used to model it. Suspension of the car in its guide rails is assumed to be rigid. In all the cases the mass of the car is denoted by m, car has a finite dimensions and the length of the cable is l. In Fig.1c, due to string modeling of the cable, the bending stiffness EI is neglected.

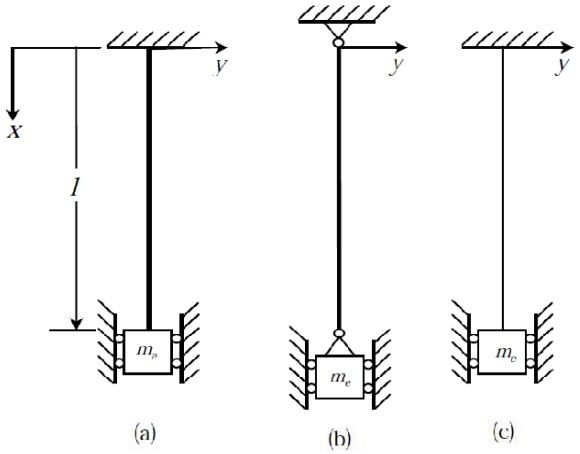

Fig. 1 Stationary hoist cable with the suspension of the car in rigid guide rails: (a) fixed–fixed beam model, (b) pinned–pinned beam model, and (c) string model

When the cable is modeled as a tensioned beam, as it illustrated in Fig.1a and Fig.1b, the governing equation of free lateral vibration is extracted as

$$\rho y_{tt}(x,t) - [P(x)y_x(x,t)]_x + EIy_{xxxx}(x,t) = 0, \quad 0 < x < l \tag{1}$$

Where the subscripts x and t denote the lateral displacement of the cable and corresponding time, respectively. ρ is the mass per unit length, l is the length of the cable, EI is the bending stiffness, and P(x) is the tension at position x given by

$$P(x) = [m_e + \rho(l - x)]g, \quad (2)$$

Where g denotes the gravity acceleration.

As shown in Fig.1a, the boundary conditions for fixed ends are

$$\begin{aligned} y(0,t) = y_x(0,t) = 0, \\ y(l,t) = y_x(l,t) = 0, \end{aligned} \quad (3)$$

Similarly, the boundary conditions for pinned ends, as shown in Fig.1(b) are

$$\begin{aligned} y(0,t) = y_{xx}(0,t) = 0, \\ y(l,t) = y_{xx}(l,t) = 0, \end{aligned} \quad (4)$$

The boundary conditions for the last model as illustrated in Fig.1(c) are

$$y(0,t) = 0, \ \ y(l,t) = 0, \quad (5)$$

For the cable models in Fig. 2(a) and (b), the boundary conditions at $x = 0$ are the same as those in (3) and (4), respectively, and the boundary conditions at $x = l$ are

$$\begin{aligned} y_{xx}(l,t) = 0 \quad (6) \\ EIy_{xx}(l,t) = P(l)y_x(l,t) + m_e y_{tt}(l,t) + c_e y_t(l,t) + k_e y(l,t) \end{aligned}$$

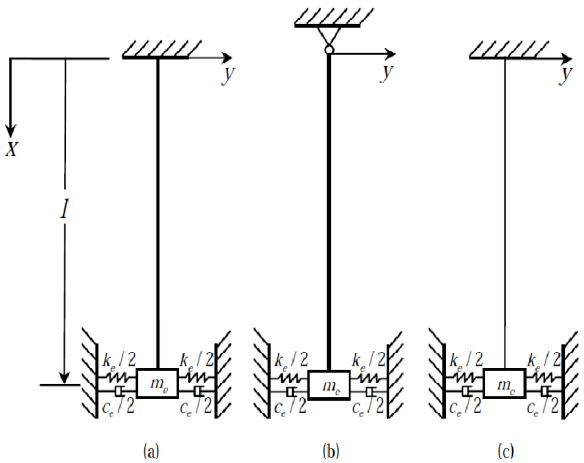

Fig. 1 Stationary hoist cable where the car is modeled as a point mass m_e and its suspension against the guide rails has a resultant stiffness k_e and damping coefficient c_e: (a) beam model with a fixed end at x = 0; (b) beam model with a pinned end at x = 0; and (c) string model

III. Analytical Solution Procedure

In this part of this paper, a brief description of an analytical technique that is going to be used to find approximate analytical solutions for vibration problem described in section 2 is given. There are many numerical but a few analytical methods for solving the nonlinear equations. In this paper variational iteration method (VIM) is used because it is a fast and easy method in finding an appropriate solution for nonlinear problems.

A. Variational Iteration Method Concept

To illustrate the basic concepts of this method, consider the following nonlinear equation:

$$L[u(x,t)] + R[u(x,t)] + N[u(x,t)] = g(x,t) \quad (7)$$

Where R is a linear operator partial derivatives with respect to x, L is the linear time derivative operator, N is a nonlinear term and $g(x,t)$ is an inhomogeneous term.

According to variational iteration method, the following correction function must be constructed:

$$u_{n+1}(x,t) = u_n(x,t) + \int_0^t \lambda[Lu_n + R\tilde{u}_n + N\tilde{u}_n - g\,]ds \quad (8)$$

Where λ is a general Lagrange multiplier which can be identified optimally via variational theory, $R\tilde{u}_n$ and $\widetilde{Nu}_n$ denote restricted variations, i.e., $\delta\tilde{u}_n = 0$.

IV. Application of the Variational Iteration Method to Find a Solution for the Governing Differential Equations

In this section, the analytical technique is employed in each of the mentioned three boundary conditions of cable vibration to gain the solutions of the governing equations.

A. Governing Equation for Fixed-Fixed Beam Model

To find a solution for the governing equation of beam with fixed boundaries, at first (1) is expanded into the following equation:

$$\begin{aligned} \rho y_{tt}(x,t) + \rho g y_x(x,t) - [m_e + \rho(l-x)]g y_{xx}(x,t) \\ + EIy_{xxxx}(x,t) = 0, \ \ 0 < x < l \end{aligned} \quad (9)$$

In developing a solution to a partial differential equation by separation of variables, one assumes that it is possible to separate the contributions of the independent variables into separate functions that each involve only one independent variable. To solve (1) by separation of variables, $y(x,t)$ can be factored:

$$y(x,t) = Y(x).T(t) \quad (10)$$

Where the function T depends only on t and the function Y depends only on x. Substituting (9) into the (1) gives

$$\begin{aligned} \rho Y(x)\ddot{T}(t) + \rho g T(t)Y'(x) - \\ [m_e + \rho(l-x)]gT(t)Y''(x) + EIT(t)Y^{(4)}(x) = 0, \\ 0 < x < l \end{aligned} \quad (11)$$

Now separate all the x's on one side and the t's on the other:

$$\frac{EIY^{(4)}(x) - [m_e + \rho(l-x)]gY''(x) + \rho gY'(x)}{\rho Y(x)} = \frac{-\ddot{T}(t)}{T(t)} \quad (12)$$

It is impossible for a function of an independent variable x to be identically equal to a function of an independent variable t unless both are constant. Therefore, for some constantλ^2, two separate ordinary differential equations are constructed as:

$$EIY^{(4)}(x) - [m_e + \rho(l-x)]gY''(x) + \rho gY'(x) - \rho\lambda^2 Y(x) = 0 \; \ddot{T}(t) + \lambda^2 T(t) = 0 \quad (13)$$

Begin by using the restrictions on the independent variable that generated the periodic functions.

In this case, that will be T(t):

$$T(t) = Asin(\lambda t) + Bcos(\lambda t) \quad (14)$$

where A and B are constants which depend on initial conditions. In (13), Y(x) could not be found easily because it is a nonlinear equation. There are many ways to find an approximate solution for nonlinear equations. Among the methods of nonlinear solution, variational iteration method is exclusive and individual. He [8] proposed the Lagrange multiplier for equations similar to (13) as $(s-t)$, thus the correction function of (13) may be constructed as:

$$Y_{n+1}(x) = Y_n(x) + \int_0^x (s-x)[EIY^{(4)}(s) - [m_e + \rho(l-s)]gY''(s) + \rho gY'(s) - \rho\lambda^2 Y(s)\,]ds \quad (15)$$

By considering the initial conditions and solving the linear part of (13), first answer will be as:

$$Y_0(x) = sin(x)^2 . sin\,(x-l)^2 \quad (16)$$

By continuing the iteration equations, following solutions for fixed boundaries obtained as:

$$Y_1(x) = \frac{1}{128}\big((32(x-l)g + 8\lambda^2)\rho - 128EI - 32gm_e\big)Cos(2l-2x) + \frac{1}{128}\Big(\big((16l-16x)g - \lambda^2\big)\rho + 256EI + 16gm_e\Big)Cos(-4x+2l) - \frac{1}{8}\rho gSin(2l-2x) + \frac{1}{32}\rho gSin(-4x+2l) + \frac{1}{128}\Big(\big((16l-32x)g + 8\lambda^2x^2 - 7\lambda^2\big)\rho - 128EI + 16gm_e\Big)Cos(2l) + \frac{1}{128}\Big(\big((-32l-32x)g + 8\lambda^2\big)\rho - 128EI - 32gm_e\Big)Cos(2x) + \frac{1}{128}\big((12g - 12x\lambda^2)\rho - 768EIx\big)Sin(2l) + \frac{1}{8}\rho gSin(2x) + \frac{1}{128}(((2l-64x)g + 16\lambda^2x^2 - 8\lambda^2)\rho + EI + \frac{1}{4}gm_e) \quad (17)$$

B. Governing Equation for Pinned-Pinned Beam Model

The solution procedure for pinned-pinned boundary conditions is the same for the previous part. Solving of the (13) begins with construction of correction function as

$$EIY^{(4)}(x) - [m_e + \rho(l-x)]gY''(x) + \rho gY'(x) - \rho\lambda^2 Y(x) = 0, \quad \ddot{T}(t) + \lambda^2 T(t) = 0 \quad (18)$$

By considering the initial conditions and solving the linear part of (23), iteration solution begins with:

$$Y_0(x) = sin(x)^3 . sin\,(x-l)^3 \quad (19)$$

By continuing the iteration equations, following solutions for pinned boundaries determined as:

$$Y_1(x) = \frac{1}{128}\big((32(x-l)g + 8\lambda^2)\rho - 128EI - 32gm_e\big)Cos(2l-2x) + \frac{1}{128}\Big(\big((16l-16x)g - \lambda^2\big)\rho + 256EI + 16gm_e\Big)Cos(-4x+2l) + \frac{1}{8}\rho gSin(2l-2x) - \frac{1}{32}\rho gSin(-4x+2l) + \frac{1}{128}\Big(\big(16gl + \lambda^2(8x^2-7)\big)\rho - 128EI + 16gm_e\Big)Cos(2l) + \frac{1}{128}\Big(\big((-32l+32x)g + 8\lambda^2\big)\rho - 128EI - 32gm_e\Big)Cos(2x) + \frac{1}{128}\big((-12g - 12x\lambda^2)\rho - 768EIx\big)Sin(2l) - \frac{1}{8}\rho gSin(2x) + \frac{1}{128}(32gl + (16x^2-8)\lambda^2)\rho + EI + \frac{1}{4}gm_e) \quad (20)$$

C. Governing Equation for String Model

The only difference between the current model and previous models is the stiffness of the beam which is neglected in string model. The governing equation of free lateral vibration for string model is as follows

$$[m_e + \rho(l-x)]gY''(x) - \rho gY'(x) + \rho\lambda^2 Y(x) = 0 \quad (21)$$

Similar to previous procedure of finding an approximate solution, correction function is constructed as

$$Y_{n+1}(x) = Y_n(x) + \int_0^x (s-x)[\big(m_e + \rho(l-s)\big)gY''(s) - \rho gY'(s) + \rho\lambda^2 Y(s)] \quad (22)$$

The most important and critical step of variational iteration method is finding the first answer of the iteration solution according to boundary conditions. For string model governing equation, iteration solution begins with:

$$Y_0(x) = sin(x)^2 . sin\,(x-l)^2 \quad (23)$$

By continuing the iteration equations, following solutions for string model determined as:

$$Y_1(x) = \frac{1}{128}\Big(\big((-32l+32x)g + 8\lambda^2\big)\rho - 32gm_e\Big)Cos(2l-2x) + \frac{1}{128}\Big(\big((16l-16x)g - \lambda^2\big)\rho + 16gm_e\Big)Cos(-4x+2l) - \frac{1}{8}\rho gSin(2l-2x) + \frac{1}{32}\rho gSin(-4x+2l) + \frac{1}{128}\Big(\big((16l-32x)g + 8\lambda^2x^2 - 7\lambda^2\big)\rho + 16gm_e\Big)Cos(2l) + \frac{1}{128}\Big(\big((-32l+32x)g + 8\lambda^2\big)\rho - 32gm_e\Big)Cos(2x) + \frac{1}{128}\big((12g - 12x\lambda^2)\rho\big)Sin(2l) + \frac{1}{8}\rho gSin(2x) + \frac{1}{128}\Big(\big((32l-64x)g + 16\lambda^2x^2 - 8\lambda^2\big)\rho + \frac{1}{4}gm_e\Big) \quad (24)$$

V. RESULTS AND DISCUSSIONS

The two numerical examples verify that the vibration problem can be solved by using He's variational iteration

method, accurately and efficiently. To validate results of current research, results of analytical solution are compared with results obtained by iterative Newmark's time integration methods. Since the governing equations are time consuming, an updating method is employed in conjunction with Picard-type iterative method. The parameters used here are: $\rho = 1.005\ kg/m, EI = 1.39\ Nm^2, m = 782\ kg, g = 9.81$ and $l = 182m$. Although both He's variational iteration method and the Newmark's time integration method are efficient and powerful methods for solving the beam problem, He's method leads to fewer calculations compared to the Newmark's time integration method.

Using the material iteration functions and various numbers of iterations, the first three natural frequencies of the models in Figs. 1 and 2 are calculated as shown in Table 1.

TABLE I
THE FIRST THREE NATURAL FREQUENCIES (IN RAD/S) OF THE MODELS IN FIGS. 1 AND 2 CALCULATED USING ARBITRARY NUMBER OF ITERATIONS FOR THE UNTENSIONED BEAM EIGENFUNCTIONS

Number of iterations		0	1	2	3	4
Fig. 1(a)	1st natural frequency	2.021	1.710	1.682	1.682	1.682
	2nd natural frequency	4.143	3.784	3.421	3.421	3.421
	3rd natural frequency	4.345	4.963	5.092	5.092	5.092
Fig. 1(b)	1st natural frequency	2.021	1.710	1.682	1.682	1.682
	2nd natural frequency	4.143	3.784	3.421	3.421	3.421
	3rd natural frequency	4.345	4.963	5.001	5.001	5.001
Fig. 1(c)	1st natural frequency	2.021	1.710	1.682	1.682	1.682
	2nd natural frequency	4.143	3.784	3.42	3.42	3.42
	3rd natural frequency	4.345	4.963	5.001	5.001	5.001
Fig. 2(a)	1st natural frequency	1.623	1.548	1.512	1.512	1.512
	2nd natural frequency	2.001	1.879	1.872	1.872	1.872
	3rd natural frequency	4.126	3.760	3.453	3.453	3.453
Fig. 2(b)	1st natural frequency	1.623	1.548	1.512	1.512	1.512
	2nd natural frequency	2.001	1.879	1.872	1.872	1.872
	3rd natural frequency	4.126	3.760	3.451	3.451	3.451
Fig. 2(c)	1st natural frequency	1.623	1.548	1.511	1.511	1.511
	2nd natural frequency	2.001	1.879	1.872	1.872	1.872
	3rd natural frequency	4.126	3.760	3.453	3.453	3.453

The trial functions for the models in Figs. 1(a), and 2(a) and (b) is referred to as the untensioned beam eigenfunctions. The values of natural frequency for fixed-fixed models are slightly higher than those of the pinned-pinned model due to rotational constraints at the fixed ends. The natural frequencies for string model are identical to those of pinned-pinned model due to small bending stiffness. If k_e approaches infinity, the natural frequencies of models with spring and damper boundary conditions would be the same as the corresponding models with rigid guide rails boundary conditions.

The initial displacements for the current models in Figs (1) and (2) for the maximum displacement of $d = 0.08$ at the point $x = 103.7m$ are shown in Fig (3).

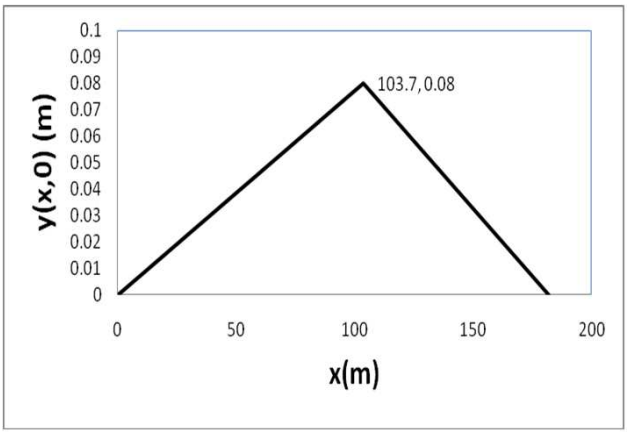

Fig. 2 The initial displacements for the models in: Figs. 1(a) and 2(a)

This initial displacement is calculated through simulating of the current models with the static deflection of a beam with the same boundary condition under uniform tension $m_e g$, subjected to a concentrated force at $x = a$ resulting in a displacement d at $x = a$, where a estimated by experimental procedures. Note that the small bending stiffness leads to the boundary layers in the deflections of the beams in the vicinity of the fixed ends and concentrated force to ensure satisfaction of the boundary and internal conditions.

Fig. 4(a) depicts the transverse force at the lower end (i.e.,$x = l$) of each model in Fig.1 under mentioned initial conditions.

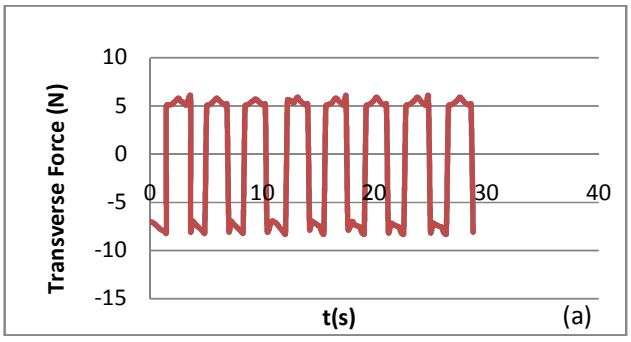

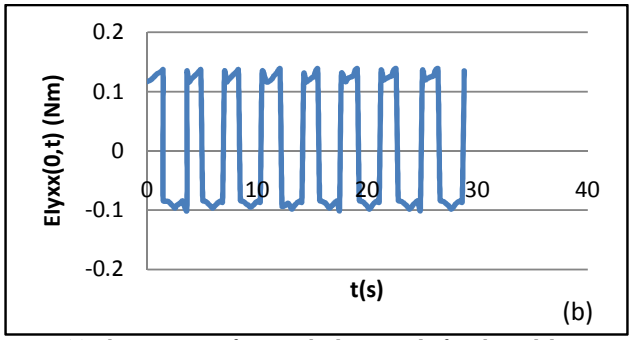

Fig. 3 (a) The transverse force at the lower end of each model in Fig. 1 under the corresponding initial displacement shown in Fig. 3 (b) The bending moment at the upper end of the model in Fig. 1(a)

While $y_x(x,t)$ induces the shear force $-EIy_{xxx}(l,t)$ at $x=l$ for the model in Fig. 1(a), term $-EIy_{xxx}(l,t)+P(l)y_x(l,t)$ for the model in Fig. 1(b) and the transverse component of tension $P(l)y_x(l,t)$ for the model in Fig. 1(c), the values of these models are the same. Fig. 4(b) shows the bending moment at the lower end of the model in fixed beam model in rigid guide rails but, the bending moment at the two ends of the fixed-fixed beam model vanishes. In both models, the bending moment at an interior point of the models is eliminated due to smaller orders of magnitude in comparison to those at the fixed ends of the model. The untensioned beam eigenfunctions can be used to determine the transverse force at an interior point of the fixed-fixed beam model and any point of the pinned-pinned model because it is dominated by the transverse component of the tension, which involves the first order derivative y_x.

Under the above initial conditions the transverse force at the upper end (i.e.,$x=l$) of each model in Fig. 2 is shown in Fig. 5(a). Similar to the case in Fig. 4(a), the transverse force at x=0; though given by different expressions, has essentially the same value for the three models. The bending moment at the upper end of the model in Fig. 2(a) is shown in Fig. 5(b).

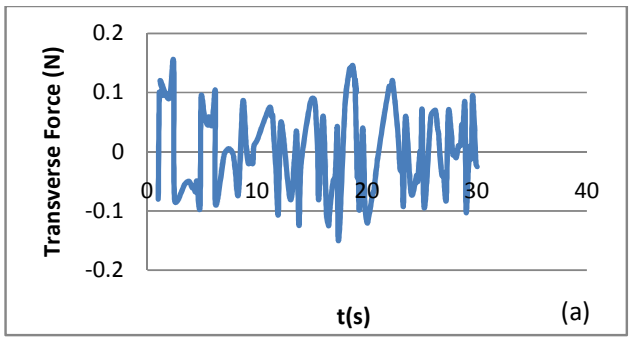

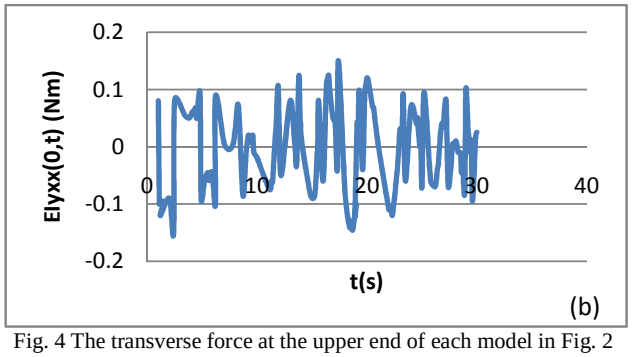

Fig. 4 The transverse force at the upper end of each model in Fig. 2 under the corresponding initial displacement shown in Fig. 3 (b) The bending moment at the upper end of the model in Fig. 2(a)

The untensioned beam eigenfunctions can be used to calculate the transverse force at an interior point of the model in Fig. 2(a) and any point of the model in Fig. 2(b). Beam eigenfunctions can be used to determine the transverse force at the lower end of the models in Fig. 2(a) and (b) because they satisfy a more realistic boundary condition, $EIy_{xxx}(l,t)=0$. The transverse force at the lower end of the model in Fig. 2(c) cannot be determined here because the trial functions satisfy$Y'(l)=0$.

VI. Conclusion

In the current paper the variational iteration method (VIM) is employed to investigate the characteristics of the free vibration of elevator cables with small bending stiffness. Responses of a dynamical system are remarkably affected by the modal responses of the system, an idea that has been led to the appearance of mode superposition techniques in determining the dynamic responses of the multi-body systems. Although behavior of stationary cables is properly predicted by the string and beam models, the maximum bending moment occurs at the fixed ends of the beam models. In addition, y_{xx} and y_{xxx} cannot be extracted for the untensioned beam eigenfunctions.

References

[1] W.D. Zhu, L.J. Teppo, Design and analysis of a scaled model of a high-rise high-speed elevator, Journal of Sound and Vibration 264 (2003) 707–731
[2] R.M. Chi, H.T. Shu, Longitudinal vibration of a hoist rope coupled with the vertical vibration of an elevator car, Journal of Sound and Vibration 148 (1) (1991) 154–159.
[3] T. Yamamoto, K. Yasuda, M. Kato, Vibrations of a string with time-variable length, Bulletin of the Japan Society of Mechanical Engineers 21 (162) (1978) 1677–1684.
[4] Y. Terumichi, M. Ohtsuka, M. Yoshizawa, Y. Fukawa, Y. Tsujioka, Nonstationary vibrations of a string with time-varying length and a mass–spring system attached at the lower end, Nonlinear Dynamics 12 (1997) 39–55.
[5] W.D. Zhu, J. Ni, Energetics and stability of translating media with an arbitrarily varying length, American Society of Mechanical Engineers Journal of Vibration and Acoustics 122 (2000) 295–304.
[6] W.D. Zhu, G.Y. Xu, Vibration of elevator cables with small bending stiffness, Journal of Sound and Vibration 263 (2003) 679–699.
[7] J.H. He, Some asymptotic methods for strongly nonlinear equations, International Journal of Modern Physics B 10 (2006) 1141-1199.
[8] J.H. He, Non-perturbative methods for strongly nonlinear problems, Dissertation. de-Verlag im Internet GmbH, 2006.